HAL
archives-ouvertes.fr

Active Thermal Shearography and Infrared Thermography Applied to NDT of Reinforced Concrete Structure by Glued CFRP

Louis-Daniel Théroux, Jean Dumoulin, Xavier Maldague

▶ To cite this version:

Louis-Daniel Théroux, Jean Dumoulin, Xavier Maldague. Active Thermal Shearography and Infrared Thermography Applied to NDT of Reinforced Concrete Structure by Glued CFRP. EWSHM - 7th European Workshop on Structural Health Monitoring, IFFSTTAR, Inria, Université de Nantes, Jul 2014, Nantes, France. hal-01020324

HAL Id: hal-01020324
https://hal.inria.fr/hal-01020324

Submitted on 8 Jul 2014

ACTIVE THERMAL SHEAROGRAPHY AND INFRARED THERMOGRAPHY APPLIED TO NDT OF REINFORCED CONCRETE STRUCTURE BY GLUED CFRP

Louis-Daniel Théroux[1], Jean Dumoulin[1,3], Xavier Maldague[2]

[1] *LUNAM Université, IFSTTAR, COSYS/SII, F-44340, Bouguenais, France*
[2] *Laval University, Departement of Electrical and Computer Engineering, LVSN/MIVIM, Av. De la Médecine, Québec (Québec), Canada*
[3] *INRIA, I4S Team, Campus de Beaulieu, 35042 Rennes cedex, France*

louis-daniel.theroux@ifsttar.fr

ABSTRACT

This research paper presents the study of thermography and shearography to evaluate CFRP reinforcement of concrete structures. The study explores the strengths and weaknesses of both non-destructive-testing (NDT) methods. It will be shown that by coupling the methods, the detection is more reliable and the defect evaluation more thorough as both the thermal and thermo mechanical properties are tested. Once the core theoretical concept regarding both methods is presented, the viability is demonstrated in the experimentation part of this study. With the experimental results confirming the feasibility of the coupling of both methods, the numerical model conceived allow to better conduct analysis that are not otherwise possible with the experimental results.

KEYWORDS : *Shearography, Active Infrared Thermography, CFRP, Thermal Excitation, NDT.*

INTRODUCTION

Over the course of the years, as concrete structures age, they tend to deteriorate which compromise their reliability. Thus, retrofitting and reparation of those structures was and still is an issue studied by many. Among the solutions found, one widely used is the gluing of CFRP sheets [1] on flawed structure. However, the efficiency of this type of reinforcement can only be certain if the bonding quality is assured. Technicians responsible for the installations of the CFRP plates are highly trained but there is always a risk that defects could be present in the bonding. In this regard, many NDT techniques were developed [2]. Among those, for ease of utilization *in situ*, it is preferable to have a method that is contactless and full field. Thermography fulfills these conditions and has been proven a reliable and efficient way to not only detect but also characterize the defect in some extent [3]. However, using thermography gives little information about how the defects impact the bonding strength. It doesn't answer the question if the detected defects compromise the efficiency of the reinforcement. To asses this matter, a testing technique that is based on the mechanical properties is required. For example, test by tearing gives a good idea of the bond's strength but is unfortunately a destructive test and is neither full field nor contactless. We turn to shearography, a NDT that gives the value of out-of-plane displacement of a surface by analysing the phase of a projected coherent light beam. The displacement must be induced in the surface by applying a strain. For conventional shearography [4], the stress is caused by applying a vacuum on the surface. Instead, this paper studies the use of a thermal excitation to induce stress. Furthermore, for ease of

implementation, thermal shearography and active infrared thermography can use the same excitation source.

1 THEORY AND FUNDAMENTAL CONCEPTS OF SHEAROGRAHPY AND THERMOGRAPHY

This section provides a brief summary on the main principles and fundamental concepts regarding active infrared thermography and shearography.

1.1 Thermal Shearography

Before explaining what shearography is, it is necessary to understand the underlining concept of holography. Holography is the measure of the phase of coherent light projected on a surface. The light reflected by the surface comes across a reference beam from the same source. The interference of both light waves, either constructive or destructive, cause variation in the light intensity. When measured, it gives the phase map of the object but it doesn't yield information on the defects unless stress is induced in the surface. By doing so, the area where defects are present will cause the surface to deform differently from the flawless regions. The approach consists of taking two phase map, one where the surface is in its normal state and another when the surface is deformed. Then, by subtracting the two phase maps, it is possible to detect the defects. In theory, this work but in practice, the setup is too sensible to noise. (Depending on the wavelength, it is sensible to deformations of approximately 1 μm.) Any vibration or change in the air refractive index cause change in the optical path length, consequently compromising the measure. To solve this problem, the reference beam and the object beam must share a similar path. The solution is to use a reference beam that is also coming from the object. The object beam is guided through a Michelson interferometer which causes the beam to interfere with a slightly sheared version of itself, thus the name shearography. Under the consideration that the light source and the point of observation are at the same location and perpendicular to the inspected surface, the relation between the phase difference and the out-of-plane displacement is [5]:

$$\Delta\varphi = k_w \left(\frac{\partial w}{\partial x}\right)\delta. \tag{1}$$

With:

$$k_w = \frac{4\pi}{\lambda} \tag{2}$$

Where $\Delta\varphi$ is the phase difference, w is the out-of-plane displacement, k_w is the wave vector, λ is the wavelength and δ is the shear distance along x. The phase extraction method with four images with intensity I_N gives the following relation:

$$\varphi = \frac{\arctan(I_4 - I_2)}{I_1 - I_3} \tag{3}$$

Coming from the resolution of the following equation using $N = 4$ and $\varphi_N = N \times 2\pi/4$:

$$I_N = I_0(1 + m \cdot \cos(\varphi + \varphi_N)) \tag{4}$$

In most past studies [6, 7], the stress induced in the surface is done by applying a depression on the surface. While this methods gives directly a precise value of the force applied, it is however only located on the surface and require a contact. In our study, the use of thermal stress present the advantage of being contactless but does to give the exact value of the stress induced. To calculate

the thermal stress, information about the temperature field distribution in the object is required, hence the use of thermography that could be coupled with inverse thermal models.

1.2   Thermography

Infrared thermography allows the measure of the apparent surface temperature of a structure. Through time, when variation in the local thermal equilibrium occurs, defects with different thermal properties than sound region affect the temperature measured. The study of the transient heat transfer regime makes possible the detection of flaws by infrared thermography. To generate a transient heat transfer regime, two methods are available. Passive thermography use natural excitation like the sun's radiation while active thermography uses artificial or forced heating [8]. For our experiment, active thermography is used and temperature measurements are made with an infrared camera. This allows contact less measurement. The governing equation for heat conduction in a solid is:

$$\rho C \frac{\partial T}{\partial t} = \nabla \cdot (k \nabla T). \tag{5}$$

2   EXPERIMENTATION

The sample used in the experimentation consists of a 0.1 m thick concrete stab with three layers of three CFRP plates glued on top of each other. The defects are disc made of polytetrafluoroethylene (PTFE) are inserted at different depth and vary in size. These discs have a thickness of 0.5 mm and simulate the absence of glue in the bonding. Normally these defects are empty hole but since it is technically difficult to make defect of air of precise thickness and size. Instead, PTFE discs are easier to insert and have roughly the same thermal conductivity of air. This is because PTFE does not chemically bond with the glue, creating a small layer of air around its boundary and thus reducing the resulting thermal conductivity.
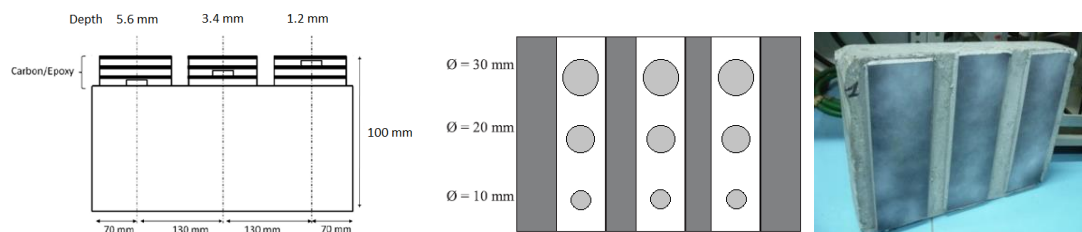

Figure 1: On the left, the schematic of the sample used in the experimentations. On the right, a photo of the sample with white paint sprayed on its surface.
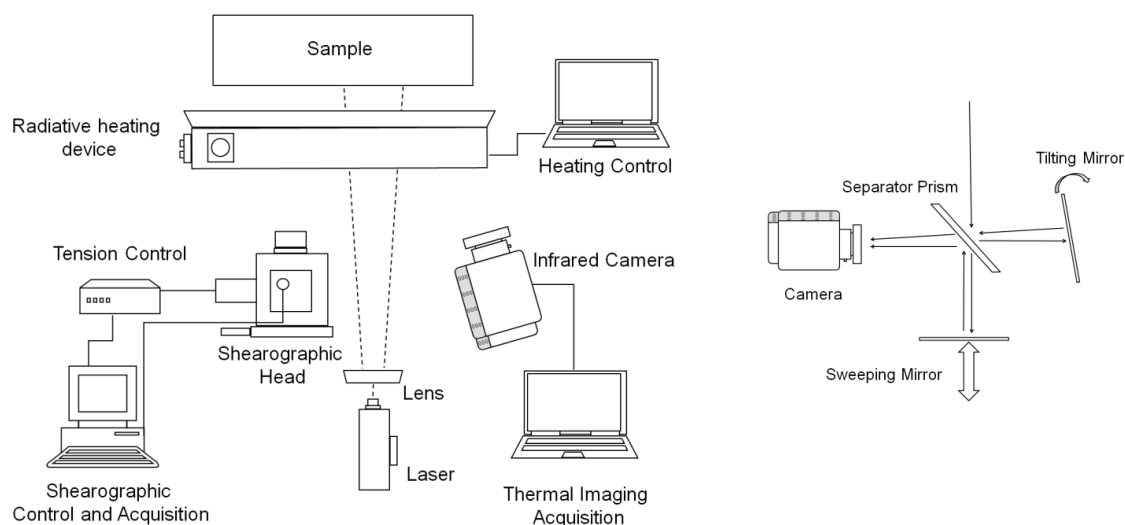
Figure 2: On the left, the schematic of the experimental setup of the simultaneous use of shearography and thermography. On the right, the detailed schematic of the shearographic head.

When using thermography and shearography simultaneously, a problem arises concerning the heating lamp. As explained earlier, shearography measure the light intensity to calculate the phase. If the heating lamp cause illumination in the same spectrum of the wavelength of the laser used (532 nm), it will be juxtaposed with the projected light beam. Thus, the shearographic measure will be either very tainted by noise or worse, simply impossible to analyse. This was the case in the initial experimentation when halogen lamps were used. Our approach to solve this problem was to use a different heat source, a carbon lamp that irradiate in the lower infrared spectrum band. This allowed shearographic measure while the sample is being heated. Another possible solution would be to use a filter for the shearographic camera.
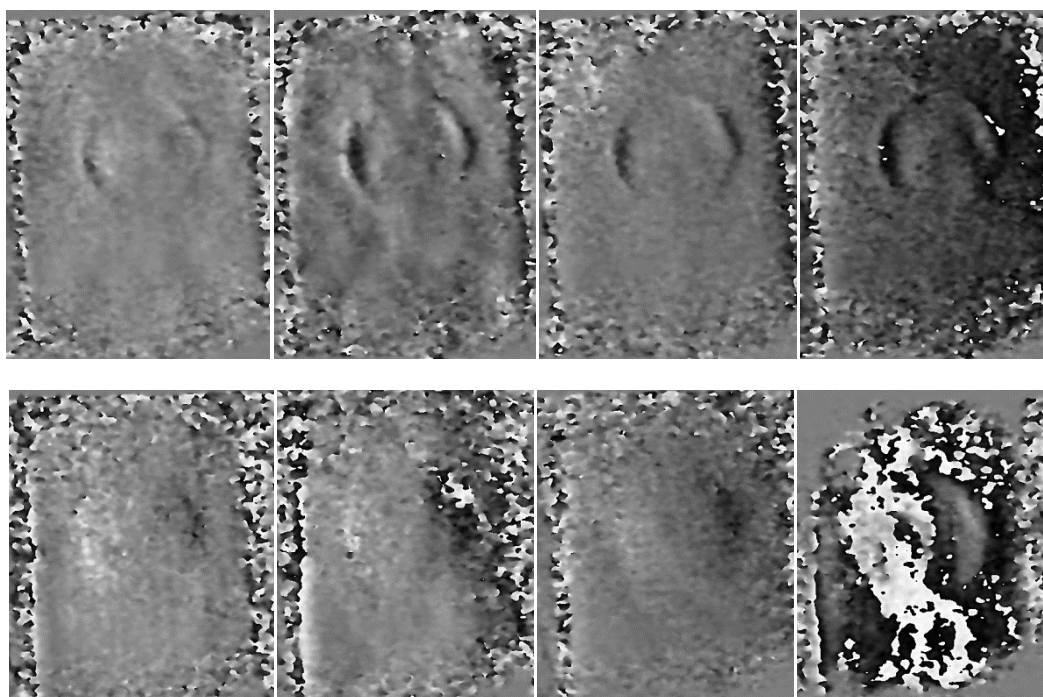

Figure 3: Shearographic images of the wrapped phase. The first three images from the left are taken during the heating while the last image was taken during the cooling.
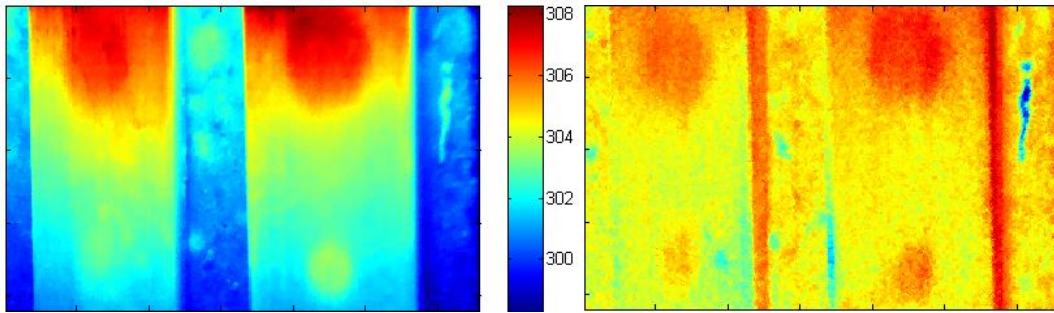
Figure 4: On the left, the raw temperature [K] and on the right, the phase map to improve defect visibility.

Results show that it was possible to detect the defects with thermography as well as with shearography. Due to limitation with the current shearographic setup, it is not possible to acquire a video sequence, only a few static images. The defect visibility is very sensible to the moments of acquisition of the phase. The reader need to recall that two phase images must be extracted. The resulting phase difference map shows the displacement difference. During the time when the first and the second phase acquisition are made, if the surface is very deformed, the multiples resulting fringes will make it difficult to unwrap the phase and the visibility may be affected as in the bottom right image of figure 3. Having a continuous phase extraction method or by increasing the phase extraction speed would allow us to observe the evolution through time of the deformation.

3   FINITE ELEMENT MODELLING OF THE SYSTEM

The geometry of the conceived model is based on the real life sample. To recreate the experimental condition of the real-life measurement, multiple conditions are applied to the model. All the elements in the model are subject to conduction heat transfer in solid as well as the linear elastic module with thermal expansion. Using the linear elastic is a valid approximation since the displacements considered in the simulation are infinitesimal. Convection cooling of 10 W/m²K is applied to the exterior faces for an ambient temperature of the air set at 20°C. To simulate the presence of the lamp, a 2 kW.m⁻² heat flux is applied on the top surface of the sample. This heat flux is conditioned by a smoothed square pulse [9] with duration of 30 seconds. The bottom surface is considered fixed. The initial temperature is set at the ambient temperature. Finally, to represent the thermal contact resistance between the glue and PTFE, a thin thermal resistance (1e-4m thick layer with conductivity of 0.0235 [w/mK]) is applied on the edges of each defect.

Table 1: Thermal and mechanical properties of materials used in the COMSOL numerical model

		Concrete	Epoxy Resin	Composite	PTFE	Air
k	[W/(m*K)]	1,8	0,2	4,2/0,7/0,7	0,235	0,02
c	[J/(kg*K)]	920	1220	1220	1050	1,0035
ρ	[kg/m³]	1200	1200	1200	2200	1,2
E	[GPa]	30	10,5	165	0,5	-
α	-	1,20E-05	2,50E-05	-8/35/35E-06	1,35E-04	-
$\vee$	-	0,2	0,33	0,33	0,46	-

3.1   Effect of nature of defect

This section concerns the study of the nature of the defect on the thermographic and shearographic measurement and how these results hold when confronting materials with different properties. As mentioned, the defects in the bonding are mostly small air layers. Since in the sample they are simulated by PTFE discs, are they a good approximation of a real defect? To answer this question,

we have taken the numerical model and replaced PTFE and replaced it with air. Furthermore, the PTFE discs were originally designed with thermal resistance. To verify this approximation, this feature was removed, but by keeping the PTFE properties.
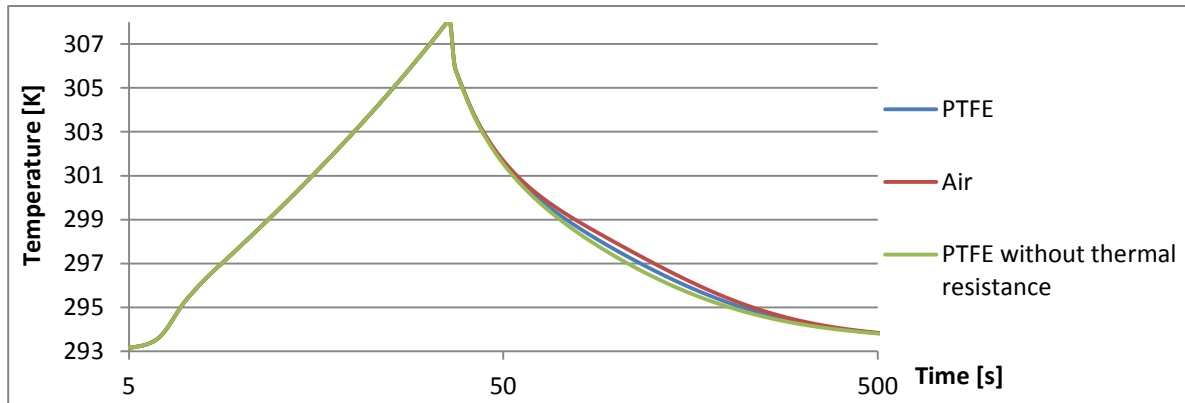

Figure 5: Graph of the temperature in function of the time for defect of different nature and properties.

From the figure 5, the temperature profile show that using PTFE with thermal resistance is a closer approximation to the behaviour of air than not using thermal resistance. However, the value of thermal used for simulation resistance may need to be tweaked to better represent the real behaviour.
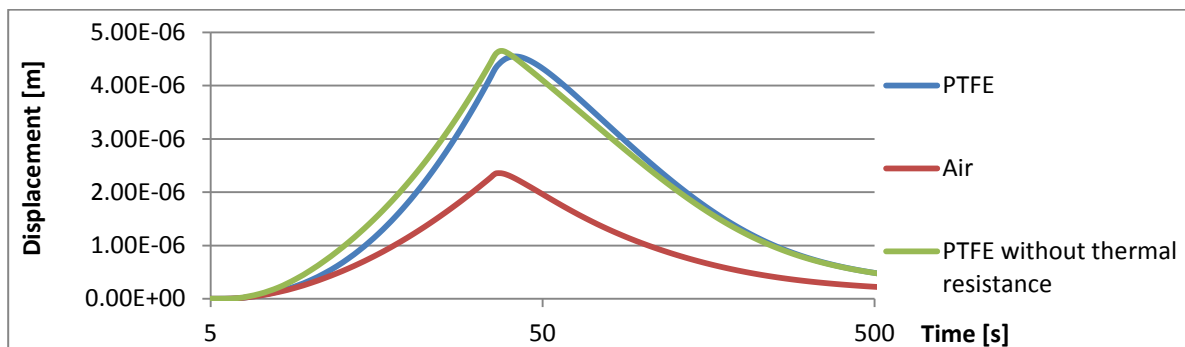

Figure 6: Graph of the out-of-plane displacement in function of the time for defect of different nature and properties.

Observing figure 6, we see that the uses of thermal resistance have little impact on the out-of-plane displacement signal. Using PTFE is not a good approximation to simulate air when taking into account the thermo mechanical behaviour. From this figure, we can also conclude that the out-of-plane displacement is more sensible to the coefficient of thermal expansion than to the temperature gradient.

3.2 Bonding Quality Analysis

An analysis on the bonding quality was conducted to better understand the relation between the thermal and thermomechanical behaviour. Ultimately, the goal is to find a way to correlate the results from shearography and thermograpy and extrapolate information about the defect. The type of information on a defect can vary from its depth, its size, its nature and mostly, how it affects the bonding.

As a reminder, it was mentioned earlier that shearography was used so it would be possible to evaluate the bonding quality. To do so, the bonding quality was compared to the raw value of the out-of-plane displacement and the time when its value reach the maximum. In the analysis, the bonding quality was determined by the ratio of the area bonded with the total area. The displacement calculated is just a mean of the out-of-plane displacement over the total area inspected.
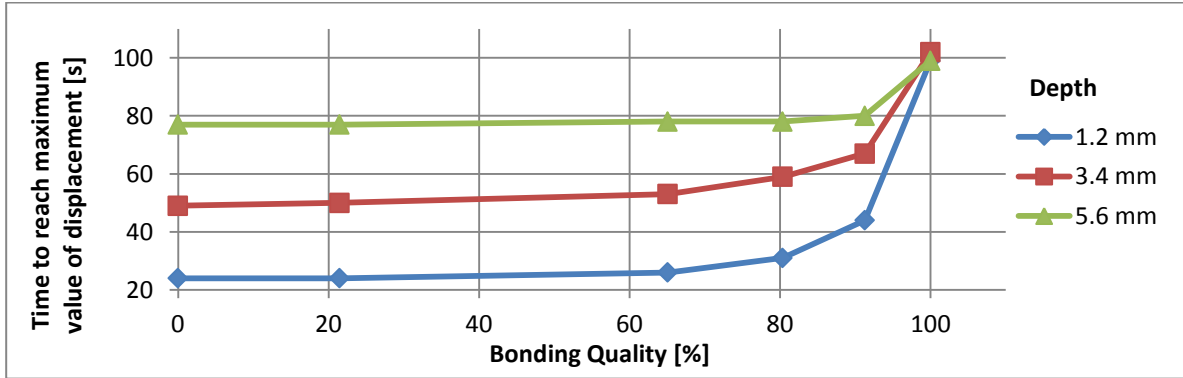

Figure 7: Graph of the time to reach the maximum value of out-of-plane displacement in function of the bonding quality for defect of various depths.

In the previous figure, it can be seen that there is a relation between the depth of the defect and the time to reach the maximum value of the displacement. This relation seems constant and valid for mid to low bonding quality (not valid for 80 to 100% bonding quality). The time to reach maximum contrast may give information on the depth of the defect, it is however not a good parameter to evaluate the quality of the bonding. For low bonding quality, the time to reach the maximum value is almost constant, no matter the depth. To evaluate the quality of the bonding, it is best to directly look at the raw out-of-plane displacement presented in the following graph.
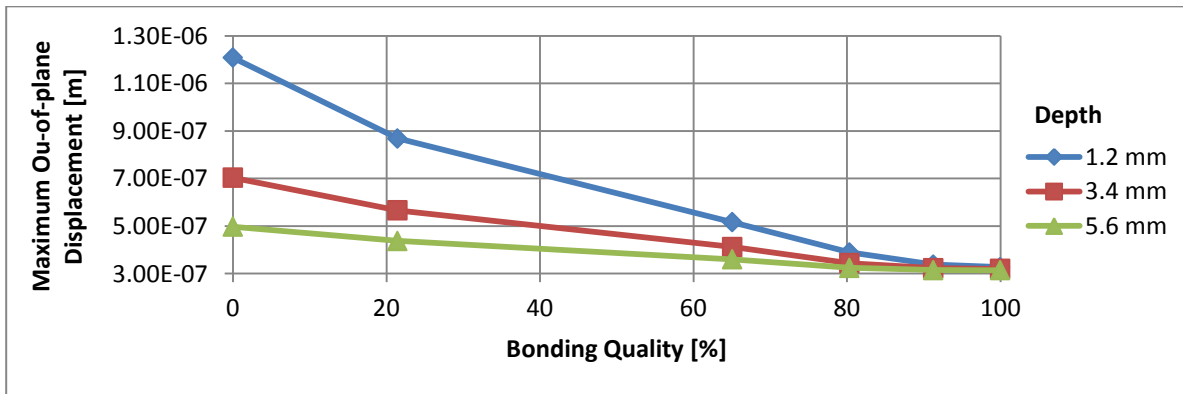

Figure 8: Graph of the maximum value of the out-of-plane displacement in function of the depth of the defects for various bonding quality.

The out-of-place displacement diminish as the defect is deeper and as the quality of the bonding increase. The deeper a defect is, the more difficult it is to distinguish the bonding quality from the value of the out-of-plane displacement. At the light of these results, the optimal evaluation process would be first to find the depth of the defect by observing the time of maximum contrast. With this information, it would be possible to calculate the bonding quality from the value of the maximum displacement.

CONCLUSION

Our study as demonstrated the feasibility of thermal shearography. Furthermore, it was demonstrated the simultaneous use of thermography and thermal shearography is not only possible but also advantageous. Among the advantage of using both systems is that both methods depend of different material proprieties. This allow coupling of the results to be a very efficient way to detect defects, no matters their nature. In the future this also means that it would make defect evaluation more trustworthy.

Multiple ameliorations to the experimental setup are possible. The first and perhaps the most important concern is the low acquisition rate (roughly 0.3 Hz) of the shearographic setup. To improve this, the whole acquisition software made under LabView must be changed. However, the acquisition rate will eventually be limited by either the camera maximum acquisition rate or the speed of the motor controlling the mirrors movements in the Michelson interferometer. If the speed limit of the electric motor is too slow, it is always possible to use a different phase extraction methods instead. For example, the continuous phase extraction, like its name imply, allow extraction of the phase while the mirror moves continuously. The maximum acquisition rate would then be limited by the time the motor takes to make a 2π dephasing.

What's interesting about thermal shearography compared to standard shearography is the ability to extract information about the defect relatively to the evolution through time of the deformation. Manipulations of the shearographic setup also reveal other limitations of the system, one of them being the area of inspection. This is mainly due to the coherent light source. Its uneven distribution makes the light distribution either too dark in the edges (like in fig 3) or too bright in the middle (the light intensity was regulated by a diaphragm). To have a evenly distributed lightning, the diffusion lens must be chosen wisely. Another aspect of the system to improve is the synchronization of the infrared camera and the shearography acquisition with the heating source. For instance, the concept of lockin thermography could be extended to the whole system.

REFERENCES

[1] R. Jain, L. Lee, *Fiber Reinforced Polymer (FRP) Composites for Infrastructure Application,* Springer, 273 pages, 2012.
[2] B.C. Ray, S.T. Hasan and D.W. Clegg, *Evaluation of Defects in FRP Composites by NDT Techniques,* in Journal of Reinforced Plastics and Composites, Volume 26, August 2007, pp 1187-1192
[3] V. Feuillet, L. Ibos, M. Fois, J. Dumoulin, Y. Candau, *Defect detection and characterization in composite materials using Pulse Thermography coupled with Singular Value Decomposition analysis and thermal quadrupole modeling*, NDT&E International, Volume 51, October 2012, pp 58–67
[4] J.W. Newman, *Aerospace NDT with Advanced Laser Shearography,* in Proceedings of 17th World Conference on Nondestructive Testing, China, 2008.
[5] Y.Y. Hung, C.Y. Liand, *Image-shearing camera for direct measurement of surface strains,* Applied Optics, vol.18, n°7, pages 1046-1051, 1979
[6] F. Taillade, M. Quiertanht, K. Benzarti, C. Aubagnac, *Shearography and pulsed stimulated infrared thermography applied to a nondestructive evaluation of FRP strengthening systems bonded on concrete structures,* Construction and Building Materials 25 2011, 568-574.
[7] T. Lamarque, *Caractérisation de délaminage par interférométrie de speckle à cisaillement avec sollicitation thermique ou mécanique,* PhD Thesis, Paris University, 1998
[8] X.P.V. Maldague, *Theory and practice of infrared technology for non-destructive testing*, John Wiley & sons Inc., 2001.
[9] A. Crinière, J. Dumoulin, C. Ibarra-Castanedo and X. Maldague , *Inverse model for defect characterization of externally glued CFRP on reinforced concrete structures: Comparative study of square pulsed and pulsed thermography*, Quantitative InfraRed Thermography Journal, Taylor & Francis Editor, 2014. DOI: 10.1080/17686733.2014.897512.